

Alkyne oligomerization catalyzed by molybdenum(0) complexes

G. Attilio Ardizzoia^{a,b,*}, S. Brenna^{a,b}, G. LaMonica^{a,b}, A. Maspero^{a,b},
N. Masciocchi^{b,c,*}

^a Dipartimento di Chimica Inorganica, Metallorganica ed Analitica, Università di Milano, Via Venezian 21, 20133 Milan, Italy

^b Dipartimento di Scienze Chimiche, Fisiche e Matematiche, Università dell'Insubria, Via Valleggio 11, 22100 Como, Italy

^c Dipartimento di Chimica Strutturale e Stereochimica Inorganica, Università di Milano, Via Venezian 21, 20133 Milan, Italy

Received 31 August 2001; accepted 5 December 2001

Abstract

Three new molybdenum(0) complexes, $[\text{Mo}(\text{CO})_5(\text{Hpz})_3]$ (**1**), $[\text{Mo}(\text{CO})_2(\text{Hpz})_2(\text{DMAD})_2]$ (**2**), (DMAD = dimethyl acetylenedicarboxylate) and $[\text{Mo}(\text{CO})_3(1\text{-Me-imidazole})_3]$ (**3**) were synthesized and characterized. Their activity and selectivity in alkyne cyclotrimerization and co-trimerization reactions was investigated. The molecular structures of **1** and **2** have been determined by unconventional *powder* and standard *single-crystal* diffraction methods, respectively. **1** consists of a pseudo-octahedral complex of C_3 symmetry, with the ligands in *fac* disposition; complex **2**, of idealized C_2 symmetry, is obtained by substitution of one CO and one pyrazole in **1** by two DMAD ligands, and shows the rare *trans* configuration of π -bound acetylenic moieties. © 2002 Published by Elsevier Science B.V.

Keywords: Molybdenum; Cyclotrimerization; Catalysis; Powder diffraction; Crystal structure

1. Introduction

In the last decades, the alkyne cyclotrimerization reaction forming benzene derivatives has been widely investigated [1,2], particularly because, through the formation of C–C bonds, new interesting products, later susceptible of further transformations, can be prepared. Several catalytic systems, based on cobalt [3], nickel [4], palladium [5] and rhodium [6] species, can promote this reaction, in heterogeneous or homogeneous conditions. Examples of alkyne polymerization and cyclotrimerization by molybdenum(II) complexes, in the presence of Lewis acids [7], or by heterobimetallic systems containing Mo–Sn [8] or Mo–Ge [9] bonds are also known. Polymerization reactions of phenylacetylene catalyzed by molybdenum(0) complexes such as $[\text{Mo}(\text{CO})_6]/\text{PhOH}$ [10] or by $[\text{ArM}(\text{CO})_3]$, (M = Cr, Mo, W) [11], have also been reported.

Recently, we began investigating the activity of molybdenum(0) species in this reaction, using ‘electron-poor’ alkynes like ethyl propiolate (EP,

$\text{EtOOC}-\text{C}\equiv\text{C}-\text{H}$) and dimethyl acetylenedicarboxylate (DMAD, $\text{CH}_3\text{OOC}-\text{C}\equiv\text{C}-\text{COOCH}_3$). To this goal, we employed $[\text{Mo}(\text{CO})_6]$ as starting material; partial ligand substitution with pyrazole and its analogues was later performed, in search of an improved catalyst activity and satisfactory products yields. Therefore, this paper report on the synthesis and characterization of these catalysts, as well as on the selectivity of the cyclotrimerization reactions derived therefrom.

2. Results and discussion

When a suspension of $[\text{Mo}(\text{CO})_6]$ in toluene under nitrogen at 60 °C was treated with excess ethyl propiolate (EP), the two possible products of cyclotrimerization, 1,2,4- and 1,3,5-tricarboethoxybenzene, were catalytically formed in an approximate 2:1 ratio (see Table 1); thus the 1,3,5-isomer is obtained in higher yields than that foreseen from purely statistical considerations. Indeed, in agreement with the mechanism proposed for alkynes cyclotrimerization [1], a (1,2,4)-versus (1,3,5)-isomer ratio of 3:1 is expected [12]. Thus, steric effects seem to be at work, as confirmed by the

* Corresponding authors. Fax: +39-031-2386119.

E-mail address: attilio.ardizzoia@uninsubria.it (G.A. Ardizzoia).

observation that $[\text{Mo}(\text{CO})_6]$ does not promote the oligomerization of diphenylacetylene, which contains two bulky, and rigid, aryl groups next to the reactive site.

Catalytic cyclotrimerization of EP was effective even in the presence of water. Moisture often causes the decomposition of the intermediate metalla-cyclopentadiene species, and only recently a catalytic system active in aqueous medium has been reported [13]. Our studies showed that the activity of $[\text{Mo}(\text{CO})_6]$ was not inhibited by H_2O , its efficiency being apparently unaltered. On the contrary, the presence of molecular oxygen in the reaction vessel dramatically lowered the yield of benzene derivatives down to about 5%, and the formation of a black precipitate, constituted by insoluble species perhaps derived from alkyne oligo- and polymerization, was observed. Similar results were observed employing dimethyl acetylenedicarboxylate (DMAD).

With the aim to improve reaction yields and selectivities, we decided to induce CO substitution on the starting $[\text{Mo}(\text{CO})_6]$ complex, thus modifying the steric and the electronic properties at the metal center. As initial choice, we selected pyrazole (Hpz), a σ -donor ligand which was expected to increase the electron density at the active site (Table 1).

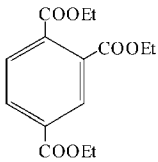
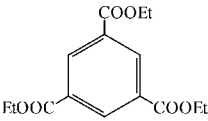
When $[\text{Mo}(\text{CO})_6]$ was suspended in heptane at 95°C and treated with excess pyrazole, a pale-yellow precipitate suddenly formed, which, on the basis of elemental analysis and spectroscopic data, was formulated as $[\text{Mo}(\text{CO})_3(\text{Hpz})_3]$ (**1**). The IR spectrum of **1** shows a

sharp absorption of medium intensity, centered at 3410 cm^{-1} , attributable to the N–H stretching of the pyrazole molecules and three strong absorptions at 1897, 1777, 1730 cm^{-1} , due to the carbonyls stretching. The pattern of these bands is in agreement with a *fac* geometry about the metal centers [14], as later confirmed by our X-ray powder diffraction analysis (reported below).

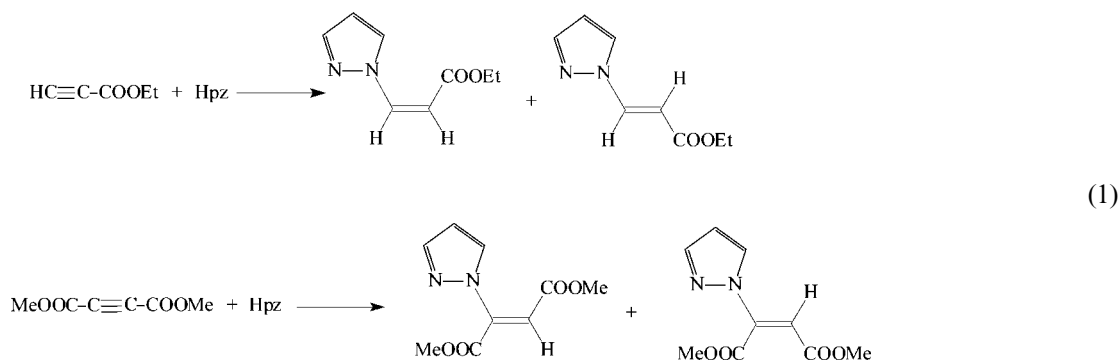
$^1\text{H-NMR}$ spectrum of **1** (acetone- d_6 , RT) showed four signals: a singlet at 12 ppm, attributed to the N–H proton (disappearing after treatment with D_2O) and three singlets in the aromatic region, centered at 7.83, 7.21 and 6.37 ppm, respectively (the pyrazole C–H protons). The separation observed for the protons in 3 and 5 position on the heteroaromatic ring, which was higher than that reported in literature [15], is probably due to the different influence of the metal center over the considered protons.

If $[\text{Mo}(\text{CO})_3(\text{Hpz})_3]$ was suspended in toluene with a 1:15 excess of alkyne (EP or DMAD), cyclotrimerization products were quickly formed. It was found necessary to operate at 60°C in order to facilitate partial pyrazole dissociation and, consequently, alkyne co-ordination and completion of the reaction. Unfortunately, the presence of dissociated pyrazole molecules promoted undesired side reactions, giving rise to the formation of both *cis* and *trans* isomers of a pyrazole-alkyne olefinic adduct, via a nucleophilic attack to the activated acetylenic triple bond Eq. (1) [16].

Table 1
Product distribution in EP cyclotrimerization

| products | catalytic system | | |
|---|-------------------------------------|--|-------------------------------------|
| | $\text{Mo}(\text{CO})_6/\text{N}_2$ | $\text{Mo}(\text{CO})_6/\text{H}_2\text{O}/\text{N}_2$ | $\text{Mo}(\text{CO})_6/\text{O}_2$ |
|  | 66% | 65% | 63% |
|  | 34% | 35% | 37% |
| total yield | 100% | 100% | 5% |

The presence of molecular oxygen reduces the yield to 5%, the percentage distribution of isomers remaining essentially constant (see text).



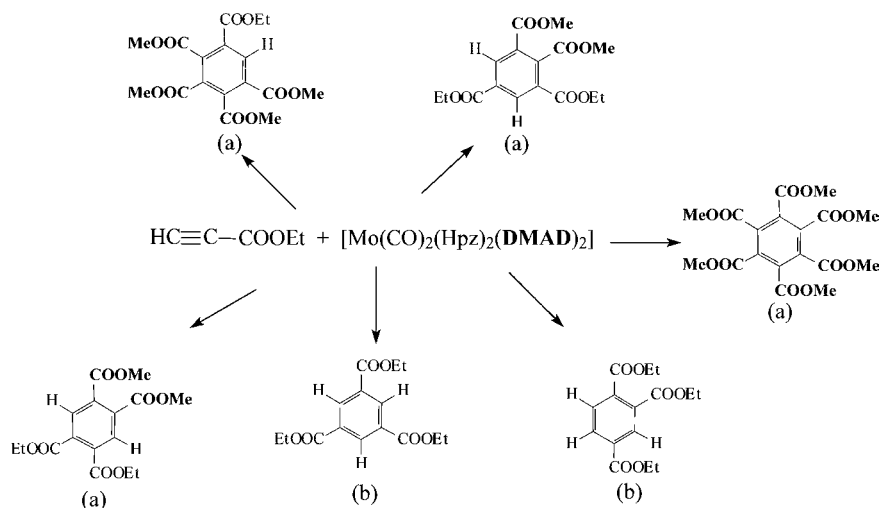
Differently, when compound **1** was dissolved at room temperature in carbon disulfide (CS_2) in the presence of DMAD, a pale yellow product was obtained. On the basis of elemental analysis and spectroscopic data, it was formulated as $[\text{Mo}(\text{CO})_2(\text{Hpz})_2(\text{DMAD})_2]$ (**2**), derived by the substitution of one carbonyl and one pyrazole ligands by two DMAD molecules. As mentioned above, the reaction of **1** with DMAD in toluene solution affords mainly cyclotrimerization products, even at room temperature; thus, isolation of **2** in CS_2 speaks for a relevant solvent effect. Additionally, we proved that $[\text{Mo}(\text{CO})_6]$, in CS_2 and in presence of excess DMAD, did not afford any reaction, thus indicating that pyrazole is indeed necessary to promote (further) ligand substitution during the formation of **2**.

The IR spectrum (nujol mulls) of $[\text{Mo}(\text{CO})_2(\text{Hpz})_2(\text{DMAD})_2]$ shows the N–H stretching of the pyrazole ligands at 3376 cm^{-1} and two sharp carbonyl stretching bands at 2011 and 1950 cm^{-1} characteristic of *cis*- $\text{Mo}(\text{CO})_2$ fragments, as observed in a number of analogue species [17].

$^1\text{H-NMR}$ of **2** (acetone- d_6 , RT) exhibits a singlet at 12 ppm attributable to the pyrazole N–H protons and three signals at 7.82, 7.47 and 6.35, respectively, assigned to 3, 5 and 4 protons of the heteroaromatic ring.

Again, as previously noted for $[\text{Mo}(\text{CO})_3(\text{Hpz})_3]$, there was a large separation between the 3 and 5 ^1H resonances. In addition, a signal at 3.77 ppm due to COOCH_3 groups of the alkynes is also present. When the spectrum was recorded at $-90\text{ }^\circ\text{C}$ (acetone- d_6) the spectral features of the pyrazole protons did not change significantly; differently, splitting of the COOCH_3 singlet of the co-ordinated DMAD molecules (3.70 and 3.76 ppm) occurs. At low temperatures, the fluxional behavior of the acetylenic ligands was probably prevented, causing the differentiation of the swinging CH_3 groups [17a]. The detailed RT molecular structure of **2** was obtained by conventional single crystal X-ray analysis.

When **2** was suspended in toluene at $60\text{ }^\circ\text{C}$ with a tenfold excess of EP, the formation of different cyclotrimerization products was observed (Scheme 1). Apart from the obvious presence of 1,2,4- and 1,3,5-tricarboethoxybenzenes (m/z 294) derived from EP cyclotrimerization, EP/DMAD co-trimerization products were formed, containing EP/DMAD fragments in 2:1 (m/z 338) and 1:2 ratio (m/z 382); moreover, the formation of hexacarbomethoxy benzene ($[\text{C}(\text{COOMe})_6]$) was noted (m/z 426). When performing the same reaction (catalytically promoted by $[\text{Mo}(\text{CO})_2(\text{Hpz})_2(\text{DMAD})_2]$)



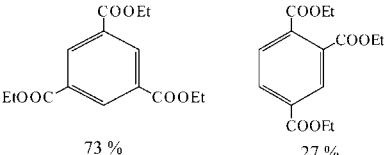
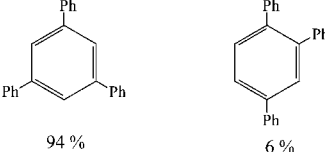
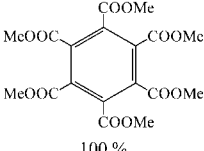
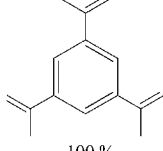
Scheme 1. Products distribution in the cyclotrimerization of EP catalyzed by complex **2**. (a) Stoichiometric amounts; (b) catalytic amounts.

with excess DMAD (rather than EP), as expected, only $[C(COOMe)]_6$ was formed. Unfortunately, also employing **2** as catalyst, the formation of alkyne-pyrazole by-products was observed (Scheme 1).

In order to avoid this problem, we decided to employ a different σ -donor ligand, which could not further act as nucleophile, such as a *N*-substituted pyrazole (or similar). However, we decided to use *N*-methyl-imidazole (1-Meim), which is more easily available than the corresponding *N*-methylpyrazole and essentially identical in terms of σ -donor ability and steric hindrance.

$[Mo(CO)_6]$ reacts with excess 1-Meim in heptane at 95° giving place to the pale yellow $[Mo(CO)_3(1-Meim)_3]$ (**3**), derivative. The IR spectrum shows three carbonyl stretching bands at 1883, 1754 and 1732 cm^{-1} . A comparison with CO bands in **1** reveals the effect of the alkyl residue on the heterocyclic nitrogen: as a consequence of the enhanced σ -donor properties of the ligand, resulting in an increased electron density on molybdenum, greater back-donation to the carbonyl ligands takes place with a lowering of the frequency of the stretching modes. 1H -NMR (acetone- d_6 , RT) evidenced a strong *pseudo*-triplet centered at 3.76 ppm, due to the different (but very close) coupling constant values with the C(2)-H and C(5)-H of the methyl protons. For the same reason, the aromatic protons give place to a convoluted series of signals in the 7.80–6.60 ppm region.

Table 2
Cyclotrimerization products formed by employing complex **3** as active species

| ALKYNE | PRODUCTS |
|---|---|
| HCC-COOEt |  73 % 27 % |
| H-C≡C-Ph |  94 % 6 % |
| MeOOC-C≡C-COOMe |  100 % |
| CHC-C(CH ₃)=CH ₂ |  ~100 % |

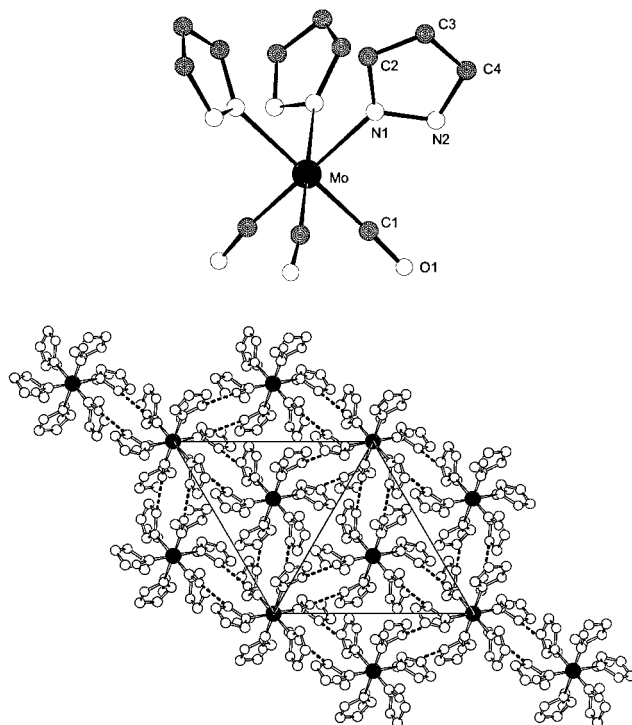


Fig. 1. Top: molecular drawing for $[Mo(CO)_3(Hpz)_3]$, with partial labeling scheme. Bottom: crystal packing, viewed down $[001]$, showing N-H \cdots O interactions (fragmented lines). Relevant bond distances (\AA) and angles ($^\circ$), with estimated S.D.'s in parentheses: Mo–N1 2.317(9), C1–Mo–C1' 84.2(7), N1–Mo–N1' 83.5(6), *cis*-C1–Mo–N1 96.1(7), *trans*-C1–Mo–N1 179.5(1), N–H \cdots O 2.753, intermolecular π - π interaction: B \cdots B 3.63 (B = pyrazole center of mass).

Among the Mo(0) species tested during this work, compound **3** resulted to be the most active in the catalytic alkyne cyclotrimerization reaction (see Table 2). This can be tentatively explained as follows: (i) the methyl residue on N(1) increases electron density on the metal, making it a better candidate in the formation M–C bonds with *electron-poor* acetylenes, such as EP and DMAD; (ii) the presence of the N-alkyl residue prevents the formation of by-products by nucleophilic attack of the nitrogen lone pair on the EP/DMAD triple bond.

2.1. Crystal structure of $[Mo(CO)_3(Hpz)_3]$ (**1**)

This complex, which lies on a crystallographic three-fold axis, consists of a molecular species bearing three carbonyls and three pyrazoles in the octahedral co-ordination mode. A schematic drawing of this complex is reported in Fig. 1, whose caption includes some relevant geometrical parameters. Thus, such Mo(0) species closely resembles already known octahedral complexes of *facial* geometry, such as $Mo(CO)_3(^3L_N)_3$ [18] (3L_N = a saturated polycyclic ligand with three donor N atoms) or, to a higher extent, $Mo(CO)_3(4\text{-Me-pyridine})_3$ [19]. Consistently, the Mo–N1 distance observed here,

2.317(9) Å, well compares to the values found for the last cited species (2.30–2.33 Å) [19]. As shown in the bottom part of Fig. 1, where the overall packing is depicted, several intermolecular hydrogen bonds are present in the solid state (N–H···O 2.753 Å), which are further accompanied by relevant π – π interactions between pyrazole rings across inversion centers of the -1 type (the distance between their centers of mass being ca. 3.6 Å). This particular disposition of the heterocyclic ring may further be stabilized by antiparallel dipolar interactions.

2.2. Crystal structure of $[\text{Mo}(\text{CO})_2(\text{Hpz})_2(\text{DMAD})_2]$ (**2**)

This complex, of idealized C_2 symmetry, consists of a molecular species bearing two mutually *cis* carbonyls and two pyrazoles *trans* to them, the remaining co-ordination sites of a pseudo-octahedral geometry being occupied by two DMAD molecules, bound through their $\text{C}\equiv\text{C}$ π electrons, *trans* to each other. An ORTEP drawing of this complex, viewed ca. down its idealized twofold axis, is reported in Fig. 2. A number of complexes bearing two substituted acetylenes (ac^*) have been structurally characterized in the past, mostly belonging to the $\text{ML}_4(\text{ac}^*)_2$ type with *cis*- ac^* units, with nearly parallel $\text{C}\equiv\text{C}$ vectors [20]. Only a few reports on *trans* ac^* moieties in $\text{ML}_4(\text{ac}^*)_2$ species have appeared, all complexes of this type showing nearly orthogonal $\text{C}\equiv\text{C}$ bonds [17]. Consistently, also $\text{Mo}(\text{CO})_2(\text{Hpz})_2(\text{DMAD})_2$ shows this latter feature, which can be attributed to the presence of d- π bonds through two competing mutually orthogonal d orbitals. Similar effects have been observed for other *trans* π -acid ligands, such CO_2 , O_2 and olefins [21]. Accordingly, rather long Mo–C distances (avg. 2.16 Å) are observed for the acetylenic carbons, if compared with those cited in ref.

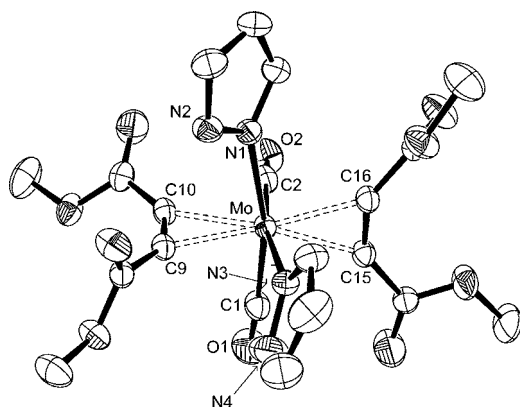


Fig. 2. ORTEP drawing of the molecular structure of $[\text{Mo}(\text{CO})_2(\text{Hpz})_2(\text{DMAD})_2]$. Relevant bond distances (Å) and angles ($^\circ$), with estimated S.D.'s in parentheses: Mo–C1 2.005(2), Mo–C2 2.008(2), C1–O1 1.135(3), C2–O2 1.135(3), Mo–C1–O1 175.9(2), Mo–C2–O2 177.6(2), Mo–N1 2.292(2), Mo–N3 2.280(3), Mo–C9 2.158(2), Mo–C10 2.178(2), C9–C10 1.277(3), Mo–C15 2.166(2), Mo–C16 2.164(2), C15–C16 1.281(3), $\text{C}\equiv\text{C}$ 139.4(2)–146.4(2) [avg. 142].

[20]. Within each acetylenic ligands, $\text{C}\equiv\text{C}$ distances (1.28 Å) and heavily bent (ca. 139–146 $^\circ$) $\text{C}-\text{C}\equiv\text{C}$ angles well agree with literature data and, in particular, closely match those reported for the $[\text{Mo}(\text{CO})_2(\text{en})(\text{DMAD})]$ analogue [17b]. However, given the paucity of structural data available for this class of compounds, we believe that the *very* small variations observed in the actual geometrical values cannot be taken as evidence of ‘disagreement between X-ray and IR spectral data’ [17b].

3. Conclusions

We reported here the synthesis and characterization of some molybdenum(0) derivatives, as well as their catalytic activity and selectivity in the alkyne cyclo-trimerization and cyclo-co-trimerization reactions. Since it has been verified that the nature of ancillary ligands plays an important role in tailoring the catalytic activity, we plan to extend this work by pursuing a systematic investigation of the steric and electronic influence of substituents on the heterocyclic rings, in a number of catalytic systems, with particular emphasis on C–C and C–N bond formation.

4. Experimental

4.1. General procedures

All solvents used were purified according to standard procedures and kept under nitrogen atmosphere. Molybdenum hexacarbonyl, pyrazole, (Aldrich) and *N*-methyl-imidazole (Merck) were used without further purification. The alkynes employed in catalytic reactions were taken from sealed bottles kept at -25 $^\circ\text{C}$ and their purity grade were confirmed by GC–MS control analysis. If not otherwise specified, all reactions were performed under an inert atmosphere of dry nitrogen. Elemental analyses (C,H,N) were carried out at the Microanalysis Laboratory of the University of Milan. IR spectra were recorded on a BIO-RAD FTS 7, ^1H -NMR were recorded on a Bruker 300. Quantitative analysis of products were performed on a Shimadzu GC-17A gas chromatograph fitted with a 30 m (0.25 mm) capillary column coupled with a Shimadzu MS QP5000 instrument.

4.2. Syntheses

4.2.1. Synthesis of $[\text{Mo}(\text{CO})_3(\text{Hpz})_3]$ (**1**)

To a solution of $[\text{Mo}(\text{CO})_6]$ (700 mg, 2.65 mmol) in heptane (20 ml), pyrazole (Hpz, 1.44 g, 21.2 mmol) was added. The solution was stirred at 95 $^\circ\text{C}$ for 8 h. During this time, a pale-yellow solid formed. The solid

was then filtered under nitrogen, washed with hot heptane and dried in a slow nitrogen flow. 73% yields. IR (nujol) 1897, 1777, 1730 cm^{-1} . Anal. Found: C, 37.44; H, 2.67; N, 21.61. Calc. for $\text{C}_{12}\text{H}_9\text{N}_6\text{O}_3\text{Mo}$: C, 37.50; H, 3.12; N, 21.87%. Upon exposure to air (few hours), powders of **1** turn violet; however, we proved by powder diffraction and IR spectroscopy that only surface oxidation takes place, the spectral features and diffraction pattern remaining substantially unchanged.

4.2.2. Synthesis of $[\text{Mo}(\text{CO})_2(\text{Hpz})_2(\text{DMAD})_2]$ (**2**) (DMAD = dimethyl acetylenedicarboxylate)

To a suspension of $[\text{Mo}(\text{CO})_3(\text{Hpz})_3]$ (120 mg, 0.31 mmol) in CS_2 (5 ml), DMAD (600 μl , 4.88 mmol), was added under stirring. After 3 h, the mixture was filtered off and the residue washed with diethyl ether, affording a yellow compound, stable in the solid state, but not in solution (84% yields). Crystals suitable for an X-ray determination were obtained by slow diffusion of diethyl ether in a dichloromethane solution of the compound. IR (nujol): 2011, 1950 cm^{-1} . Anal. Found: C, 42.12; H, 3.41; N, 9.56. Calc. for $\text{C}_{20}\text{H}_{20}\text{N}_4\text{O}_{10}\text{Mo}$: C, 41.96; H, 3.50; N, 9.79%.

4.2.3. Synthesis of $[\text{Mo}(\text{CO})_3(1\text{-Me-im})_3]$ (**3**)

1-Methyl imidazole (1.5 ml, $d = 1.03$, 18.8 mmol), dissolved in 0.5 ml of degassed heptane, was added to a solution of $[\text{Mo}(\text{CO})_6]$ (600 mg, 2.27 mmol) in heptane (20 ml). The solution was kept at 95 $^\circ\text{C}$ for 4 h; it was then slowly cooled to room temperature (r.t.) and heptane was removed under reduced pressure. The yellow residue was treated with degassed methanol (20 ml) and then filtered over a septum. The complex was dried under a nitrogen flow. 83% yields. Anal. Found: C, 45.16; H, 4.44; N, 19.28. Calc. for $\text{C}_{15}\text{H}_{18}\text{N}_6\text{O}_3\text{Mo}$: C, 45.25; H, 4.22; N, 19.72%.

4.3. Catalytic reactions

4.3.1. Cyclotrimerization of dimethyl acetylenedicarboxylate (DMAD) and ethyl propiolate (EP) by $[\text{Mo}(\text{CO})_6]$

In a Schlenk tube containing degassed toluene (5 ml) $[\text{Mo}(\text{CO})_6]$ (120 mg, 0.454 mmol) was added under stirring. The system was thermostated at 70 $^\circ\text{C}$ obtaining a clear solution. The appropriate alkyne, previously degassed with nitrogen, was then added (Mo:alkyne molar ratio 1:18). The reaction was monitored by GC–MS analysis, which revealed the presence of the cyclotrimerization products. The complete conversion of the starting alkyne is attained after about 8 h.

4.3.2. Cyclotrimerization of ethyl propiolate (EP) by $[\text{Mo}(\text{CO})_6]$ in the presence of H_2O

In a 50 ml flask, a solution of toluene (10 ml) and water (10 ml) was stirred vigorously for 15 min. Then

the two phases were separated and 6 ml of wet toluene were transferred to a Schlenk tube and degassed under nitrogen. Then, $[\text{Mo}(\text{CO})_6]$ (75 mg, 0.284 mmol) and EP (100 μl , $d = 0.968$, 0.988 mmol) were added to the solution and heated to 60 $^\circ\text{C}$ for 24 h under a bleed of wet nitrogen.

4.3.3. Cyclotrimerization of ethyl propiolate (EP) by $[\text{Mo}(\text{CO})_6]/\text{O}_2$

To a suspension of $[\text{Mo}(\text{CO})_6]$ (75 mg, 0.284 mmol) in toluene (6 ml) previously degassed with molecular oxygen, ethyl propiolate was added (100 μl , $d = 0.968$, 0.988 mmol). The suspension, kept under O_2 atmosphere, was heated to 60 $^\circ\text{C}$ for 8 h.

4.3.4. Alkyne cyclotrimerization in the presence of $[\text{Mo}(\text{CO})_3(\text{Hpz})_3]$ (**1**), $[\text{Mo}(\text{CO})_2(\text{Hpz})_2(\text{DMAD})_2]$ (**2**) or $[\text{Mo}(\text{CO})_3(1\text{-Me-im})_3]$ (**3**)

In a typical experiment, the appropriate complex was dissolved in toluene (5 ml) and treated with an excess of alkyne (Mo:alkyne ratio 1:10) at 60 $^\circ\text{C}$ for 5 h. All reactions were monitored by means of GC–MS, and found complete within 8 h.

4.3.5. X-ray powder diffraction analysis [22] of $[\text{Mo}(\text{CO})_3(\text{Hpz})_3]$ (**1**)

The gently ground powders were cautiously deposited in the hollow of an aluminium holder equipped with a zero background plate (supplied by *The Gem Dugout*, State College, PA). Diffraction data (Cu– K_α , $\lambda = 1.5418 \text{ \AA}$) were collected on a vertical scan PW1820 diffractometer, equipped with parallel (Soller) slits, a secondary beam curved graphite monochromator, a Na(Tl)I scintillation detector and pulse height amplifier discrimination. The generator was operated at 40 KV and 40 mA. Slits used: divergence 1.0 $^\circ$, antiscatter 1.0 $^\circ$ and receiving 0.2 mm. Nominal resolution for the present set-up is 0.14 $^\circ$ 2θ (FWHM) for the Si(111) peak at 28.44 $^\circ$ (2θ). A long overnight scan was performed with $5 < 2\theta < 105^\circ$, with $t = 10 \text{ s}$ and $\Delta 2\theta = 0.02^\circ$. Indexing, using TREOR [23], of the low angle diffraction peaks suggested a trigonal cell of approximate dimensions $a = 12.69$, $c = 16.54 \text{ \AA}$ $\{M(20) = 38$ [24]; $F(20) = 57$ [25] (0.006, 64)}. Systematic absences indicated, among others, $R\bar{3}$ as the probable space group, later confirmed by successful solution and refinement. Structure solution was initiated by using EXPO [26], which afforded the location of the metal atom and of some lighter atoms. Difference Fourier syntheses and geometrical modeling later afforded approximate co-ordinates for the remaining non-hydrogen atoms. The final refinements were performed with the aid of the GSAS suite of programs [27], by imposing geometric constraints to the pyrazole rings (C–C and C–N were given average literature values of 1.38 \AA , and internal ring angles fixed at 108 $^\circ$). Soft restraints were also applied to Mo–C and C–O distances [2.0 and 1.15 \AA , respectively]. The peak

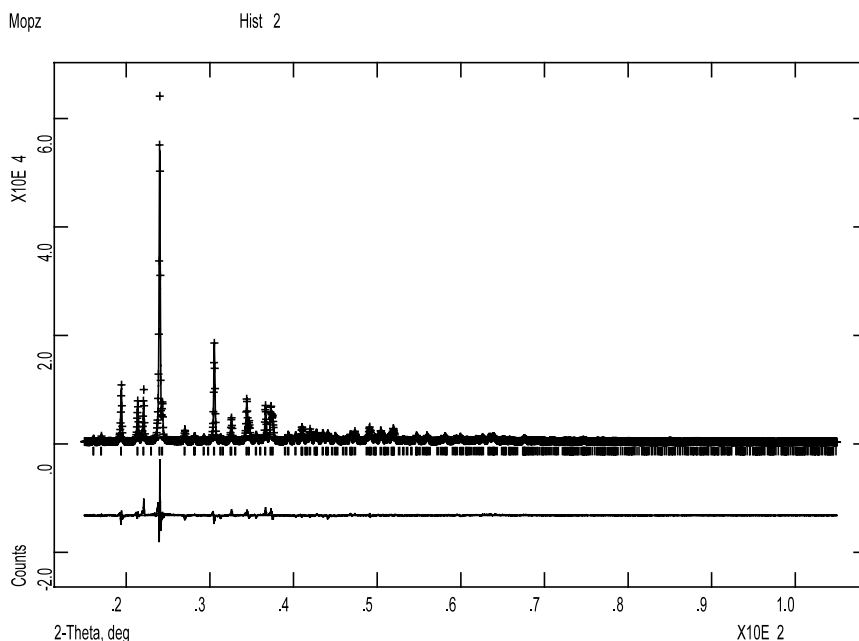


Fig. 3. Rietveld refinement plot for $[\text{Mo}(\text{CO})_3(\text{Hpz})_3]$, with peak markers and difference plot at the bottom.

shapes were best described by the Thompson/Cox/Hastings formulation [28] of the pseudo Voigt function, with GV and LY set to zero. The background function was described by a cosine Fourier series, while systematic errors were corrected with the aid of a sample-displacement angular shift; a single (refinable) isotropic displacement parameter $[U_{\text{iso}}(\text{Mo})]$ was assigned to molybdenum, while lighter atoms U's were arbitrarily given $[U_{\text{iso}}(\text{Mo}) + 0.02] \text{ \AA}^2$ values. The contribution of the hydrogen atoms to the scattered intensity was neglected. Scattering factors, corrected for real and imaginary anomalous dispersion terms were taken from the internal library of GSAS.

Crystal data: $\text{C}_9\text{H}_8\text{MoN}_4\text{O}_3$, fw 316.13 g mol^{-1} ; trigonal, $R\bar{3}$, $a = 12.6982(3)$, $c = 16.5385(7) \text{ \AA}$, $U = 2309.4(1) \text{ \AA}^3$, $Z = 6$, $\rho_{\text{calc}} = 1.364 \text{ g cm}^{-3}$; R_p and $R_{\text{wp}} = 0.085$ and 0.111 , respectively, for 4500 data points (588 independent reflections, $R_F = 0.095$) collected in the $15 < 2\theta < 105^\circ$ range. Fig. 3 shows the final Rietveld refinement plot for $[\text{Mo}(\text{CO})_3(\text{Hpz})_3]$.

4.3.6. Single crystal X-ray structure determination of $[\text{Mo}(\text{CO})_2(\text{Hpz})_2(\text{DMAD})_2]$ (**2**)

A yellow prismatic crystal of approximate dimensions $0.30 \times 0.12 \times 0.08 \text{ mm}$ was mounted on a tip of a glass fiber and put onto a goniometer head. The intensity data were collected at r.t. on an Enraf–Nonius CAD4 automated diffractometer. A least-squares fit of 25 randomly oriented intense reflections with θ ranging from 10 to 15° provided the unit cell parameters. Intensities were collected using a variable scan-range

with a 25% extension at each end for background determination. Three standard reflections were measured at regular intervals and showed no decay of the scattering power over the data collection period. Data were corrected for Lorentz, polarization and absorption (ψ -scan) effects. Structure solution by Direct (SIR97) and conventional Fourier difference methods; refinement by full-matrix least-squares using SHELX97 and the physical constants tabulated therein. Anisotropic thermal parameters were assigned to all non-hydrogen atoms. The hydrogen atoms contribution to the scattering factors was included in the last cycles in the riding model.

Crystal data: $\text{C}_{20}\text{H}_{20}\text{MoN}_4\text{O}_{10}$, fw 572.34 g mol^{-1} ; triclinic, $P\bar{1}$, $a = 8.660(1)$, $b = 10.320(1)$, $c = 13.822(3) \text{ \AA}$, $\alpha = 81.95(1)$, $\beta = 76.69(1)$, $\gamma = 85.82(1)^\circ$, $U = 1189.3(3) \text{ \AA}^3$, $Z = 2$, $\rho_{\text{calc}} = 1.598 \text{ g cm}^{-3}$; R_1 and $wR_2 = 0.025$ and 0.059 , respectively, for 4167 independent reflections collected in the $3 < \theta < 25^\circ$ range.

5. Supplementary material

Crystallographic data for the structural analyses reported above have been deposited with the Cambridge Crystallographic Data Center, CCDC no. 167916, and 167917, for compounds **1** and **2**, respectively. Copies of this information may be obtained free of charge from: The Director, CCDC, 12 Union Road, Cambridge, CB2 1EZ UK (Fax: (int. code) +44-1223-336-033; e-mail: deposit@ccdc.cam.ac.uk or www: <http://www.ccdc.cam.ac.uk>).

Acknowledgements

We thank the Italian Consiglio Nazionale delle Ricerche (CNR) and MURST for funding. We also acknowledge financial support from ICDD-International Center for Diffraction Data.

References

- [1] N.E. Schore, Chem. Rev. 88 (1988) 1081.
- [2] S. Saito, Y. Yamamoto, Chem. Rev. 100 (2000) 2901.
- [3] R.J. Baxter, G.R. Knox, J.H. Moir, P.L. Pauson, M.D. Spicer, Organometallics 18 (1999) 206.
- [4] N. Mori, S. Ikeda, Y. Sato, J. Am. Chem. Soc. 121 (1999) 2722.
- [5] A. Takeda, A. Ohno, I. Kadota, V. Gevorgyan, Y. Yamamoto, J. Am. Chem. Soc. 119 (1997) 4547.
- [6] (a) C. Bianchini, D. Masi, A. Meli, M. Peruzzini, A. Vacca, Organometallics 10 (1991) 636;
(b) W. Baidossi, N. Oren, J. Blum, H. Schumann, H. Hemling, J. Mol. Cat. 85 (1993) 153.
- [7] A. Keller, R. Matusiak, J. Mol. Cat. A 142 (1999) 317.
- [8] T. Szymanska-Buzar, T. Glowiak, J. Organomet. Chem. 575 (1999) 98.
- [9] T. Szymanska-Buzar, T. Glowiak, I. Czelusniak, J. Organomet. Chem. 585 (1999) 215.
- [10] H.C.M. Vosloo, J.A.K. du Plessis, J. Mol. Cat. 79 (1993) 7.
- [11] M.F. Farona, P.A. Lofgren, P.S. Woon, J. Chem. Soc. Chem. Comm. (1974) 246.
- [12] For asymmetric alkynes, depending on the head-to-head, head-to-tail or tail-to-tail coupling, a total of $2^3 = 8$ statistical configurations can be envisaged, which result in two isomers in 6:2 (asym:sym) ratio.
- [13] M.S. Sigman, A.W. Fatland, B.E. Eaton, J. Am. Chem. Soc. 120 (1998) 5130.
- [14] R.J. Angelici, F. Basolo, A.J. Poe, J. Am. Chem. Soc. 85 (1963) 2215.
- [15] M.A. Angaroni, G.A. Ardizzioia, T. Beringhelli, G. D'Alfonso, G. La Monica, N. Masciocchi, M. Moret, J. Organomet. Chem. 363 (1989) 409.
- [16] H. Reimlinger, C.H. Moussebois, Chem. Ber. 98 (1965) 1805.
- [17] (a) T.Y. Hsiao, P.L. Kuo, C.H. Cheng, C.Y. Cheng, S.L. Wang, Organometallics 12 (1993) 1094;
(b) C.H. Lai, C.H. Cheng, C.Y. Cheng, S.L. Wang, J. Organomet. Chem. 147 (1993) 458.
- [18] (a) R.W. Hay, I. Fraser, G. Ferguson, J. Chem. Soc. Dalton Trans. (1989) 2183;
(b) S.P. van Kouwenberg, E.H. Wong, G.R. Weisman, E.J. Gabe, F.I. Lee, P. Jackson, Polyhedron 8 (1989) 2333;
(c) G. Haselhorst, S. Stoetzel, A. Strassburger, W. Walz, K. Wiegardt, B. Nuber, J. Chem. Soc. Dalton Trans. (1993) 83;
(d) N.L. Armanasco, M.V. Baker, M.R. North, B.W. Skelton, A.H. White, J. Chem. Soc. Dalton Trans. (1998) 1145.
- [19] D.A. Schut, D.R. Tyler, T.J.R. Weakley, J. Chem. Cryst. 26 (1996) 235.
- [20] J.L. Templeton, Adv. Organomet. Chem. 29 (1989) 1.
- [21] See for example: (a) R. Alvarez, E. Carmona, J.M. Marin, M.L. Poveda, E. Gutierrez-Puebla, A. Monge, J. Am. Chem. Soc. 108 (1986) 2286;
(b) B. Chevrier, Th. Diebold, R. Weiss, Inorg. Chim. Acta 19 (1976) L57;
(c) E. Carmona, J.M. Marin, M.L. Poveda, J.L. Atwood, R.D. Rogers, J. Am. Chem. Soc. 105 (1983) 3014;
(d) C.H. Lai, C.H. Cheng, W.C. Chou, S.L. Wang, Organometallics 12 (1993) 1105.
- [22] Exploratory measurements on powders of **1** indicated its high symmetry and, consequently, the accessibility of meaningful structural results also from X-ray powder diffraction data [N. Masciocchi, A. Sironi, J. Chem. Soc. Dalton Trans. (1997) 4643].
- [23] P.E. Werner, L. Eriksson, M. Westdahl, J. Appl. Crystallogr. 18 (1985) 367.
- [24] P.M. De Wolff, J. Appl. Crystallogr. 1 (1968) 108.
- [25] G.S. Smith, R.L. Snyder, J. Appl. Crystallogr. 12 (1979) 60.
- [26] A. Altomare, M.C. Burla, G. Cascarano, C. Giacovazzo, A. Guagliardi, A.G.G. Moliterni, G. Polidori, J. Appl. Crystallogr. 28 (1995) 842.
- [27] A.C. Larson, R.B. Von Dreele, LANSCE, MS-H805, Los Alamos National Laboratory, New Mexico, 1990.
- [28] P. Thompson, D.E. Cox, J.B. Hastings, J. Appl. Crystallogr. 20 (1987) 79.